Research on Engineering Structures & Materials
www.jresm.org
Research Group

Research Article

Influence of IRC vehicular loads on seismic response of composite I-Girder bridge

Aashish Prasad Khanal [*,a], Kaushal Raj Thakur [b], Srinivasa Rao Killamsetti [c]

Dept. of Civil Engineering, Andhra University College of Engineering (A), Visakhapatnam, A.P., India

Article Info

Article History:

Received 31 Oct 2025

Accepted 15 Feb 2026

Keywords:

Composite I-girder bridge;
Seismic response;
IRC vehicular loads;
Response spectrum analysis;
Time-history analysis

Abstract

Heavy vehicles are often present on bridges during earthquakes, potentially affecting the seismic response of the structure. This study investigates the seismic behavior of a single span, two lane steel-concrete composite I-girder bridge subjected to vehicular loads specified by the Indian Roads Congress (IRC) in combination with seismic excitations. A finite-element model is developed using MIDAS Civil and validated in accordance with IRC provisions. Response spectrum analyses are conducted for Indian seismic Zones IV and V, along with linear time history analyses using recorded ground motions from the Bhuj (2001), Chamoli (1999), and India–Burma Border (1995) earthquakes. Stationary vehicular loads, including IRC Class A, Class AA, Class 70R, and Special Vehicle configurations, are applied at mid-span to obtain critical structural responses. The results indicate that stationary vehicles increase shear force, bending moment, and mid-span deflection, with heavier axle loads and closer axle spacing producing greater amplification. Seismic demands in Zone V are approximately 50% higher than those in Zone IV. Time history analyses show that the near-field Chamoli record generates responses up to three times greater than those from the Bhuj and India–Burma Border events. Overall, the findings demonstrate a non-linear relationship between axle load and seismic response, highlighting that both load magnitude and axle configuration significantly influence the dynamic demand.

© 2026 MIM Research Group. All rights reserved.

1. Introduction

Bridges are crucial to transportation infrastructure, and it is very necessary that they are reliable to handle multiple stress, especially the combined effects of heavy vehicular loading and seismic events. Traditionally, design standards have assessed the impacts of live loads and earthquake forces separately, often neglecting their simultaneous occurrence because of assumptions about low joint probability and the dominance of dead loads in seismic response [1-3]. However, past earthquake events have shown that automobiles can be present on bridges during seismic activity, which can significantly alter dynamic performance of a bridge and post-event serviceability [4,5].

Recent studies show that truck weight, axle configuration, and gross vehicle load directly affect bridge deterioration, fatigue, and the maintenance and renewal costs [6]. This highlights the importance of understanding how vehicular load impacts both existing and new bridge infrastructure. Furthermore, composite I-girder bridges are becoming more common because of their structural advantages, and they face changing requirements as heavier vehicles and complex traffic patterns become usual [7]. A specific challenge involves understanding the dynamics of interaction: advanced experimental, analytical, and numerical investigations indicate that vehicle-bridge interaction (VBI) can either enhance or reduce seismic response depending on factors such as mass distribution, vehicle modeling, and load position [2-4].

*Corresponding author: aashishprasadkhanal@gmail.com
[a]orcid.org/0009-0005-1930-3209; [b]orcid.org/0009-0008-9723-7480; [c]orcid.org/0000-0001-5764-2758
DOI: http://dx.doi.org/10.17515/resm2026-1311st1031rs

Experimental as well as finite element analyses show that the dynamic correlation between vehicle movement and bridge superstructures, including inertia and damping effects, can significantly affect the seismic fragility and reliability of steel and composite bridges [1,2,8]. This effect is strongest when a stationary vehicle is positioned at the critical mid-span, where bending moment and deflection usually reach their maximum value [1, 3-5]. The presence of this concentrated load changes the distribution of static forces in the bridge and can also influence its dynamic and seismic behavior [3-5]. Notably, live load may act as a mass damper, reducing substructure forces under certain conditions, although excessive seismic excitation could reverse this advantage [3].

The response of bridge structures is influenced by factors such as geological structures and fault characteristics, which vary significantly across regions [9]. Near-fault ground motions lead to stronger amplification than far-field motions [8,10]. Wave passage effects and soil structure interaction further raise seismic demand, with the largest impact on soft soils and sites with low apparent wave velocities [11]. This highlights the necessity to examine the response of a structure on different seismic events or conditions.

The Indian Roads Congress (IRC) defines vehicle types and load levels based on Indian traffic conditions. This approach leads to live load models and combinations that differ from the more generalized design vehicles and load models adopted in AASHTO and Eurocode [12-14]. While AASHTO and Eurocode adopt site-specific spectra that more thoroughly account for soil-structure interaction and local amplification effects [15,16], Indian codes rely on zone-based response spectra with comparatively lower design acceleration values [12]. These variations underscore the importance of evaluating bridge and structural performance under Indian loading and seismic conditions.

Despite advances, established guidance remains inconsistent, making it difficult to incorporate live loads in seismic design [3]. Considering changing traffic demands and variations among seismic design codes regarding live loads, it is crucial to understand how a stationary vehicular load at mid-span affects shear force, bending moment, and deflection during earthquakes [1,3]. This article addresses this need by investigating these critical structural responses in single span composite I-girder bridges incorporating stationary IRC vehicular loads at mid-span and thereby providing insights to advance analysis, design, and reliability assessments for seismically active regions.

2. Objectives of the Study

This study evaluates how Indian Roads Congress (IRC) vehicle loads affect the seismic performance of a 25 m single span, two lane steel-concrete composite I-girder bridge. Using finite element modeling and IRC guidelines, response spectrum analyses for zones IV and V and linear time history analyses with three Indian ground motions (Bhuj 2001, Chamoli 1999, India–Burma Border 1995) are conducted, including effects from IRC Class A, Class AA (tracked), Class 70R (wheeled), and special vehicles. The primary objectives of present study are;

- To compute and compare key response quantities for each case: shear force, bending moment and mid-span deflection.
- To identify and interpret patterns how the presence of heavy vehicles influences the seismic demands on the composite span.

3. Methodology

3.1. Modelling and Validation

A finite element model of a composite I-girder bridge is developed as per IRC guidelines and checked for the validation of the serviceability conditions. The material properties, section properties, boundary and loading conditions used for modeling and validation are discussed as follows.

3.1.1. Material Properties

For the current model, structural steel of grade E350 is selected for main girders and other steel components such as cross bracing. For concrete components such as deck slab and crash barrier,

reinforced concrete of grade M40 is defined with reinforced steel Fe500. The properties of composite section are illustrated in Table 1.

Table 1 Material properties

Property	Structural Steel	Reinforced Concrete
Grade	E350	M40
Young's modulus (E)	2.0×10^5 MPa	33,345 MPa
Poisson's ratio (ν)	0.3	0.2
Density	76.98 kN/m^3	25.49 kN/m^3
Characteristic strength	350 MPa (Yield Strength, Fy)	40 MPa (Compressive Strength, fck)
Thermal expansion coefficient	1.2×10^{-5} /°C	1.2×10^{-5} /°C

3.1.2. Time Dependent Material Properties

Time dependent material properties make it possible to examine long-term effects, particularly in concrete, such as creep, shrinkage and aging of stiffness. These phenomena are considered for modeling to ensure accurate construction-stage and long-term service life analyses. The creep, shrinkage and compressive strength for the present model is defined as per IRC 112, 2011 considering relative humidity 70% and normal cement.

3.1.3. Section Properties

Section properties define the geometric characteristics of the structural elements. These properties are basics for the accurate analysis and design of structural members as they directly influence parameters like stiffness, load-carrying capacity, deflection, and stress distribution. The geometric configuration and sectional details of the composite I-girder bridge, including the superstructure layout, composite section properties, and deck slab dimensions, are illustrated in Figures 1–4. and summarized in Table 2.

Table 2 Section properties

Parameters	Properties
Bridge deck	Reinforced concrete slab
Girders	Steel-plate girder
Span	25 m
Clear width of road way	7.5 m
Footpath	1.25 m on either side
Spacing of main girders	2 m
Cross bracing	4 @ 5 m

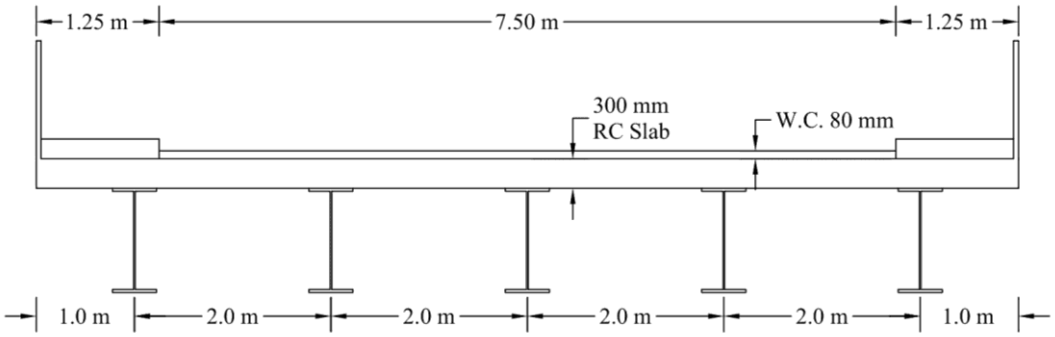

Fig. 1. Cross-sectional arrangement of the composite I-girder bridge superstructure showing deck slab, girders, and roadway configuration

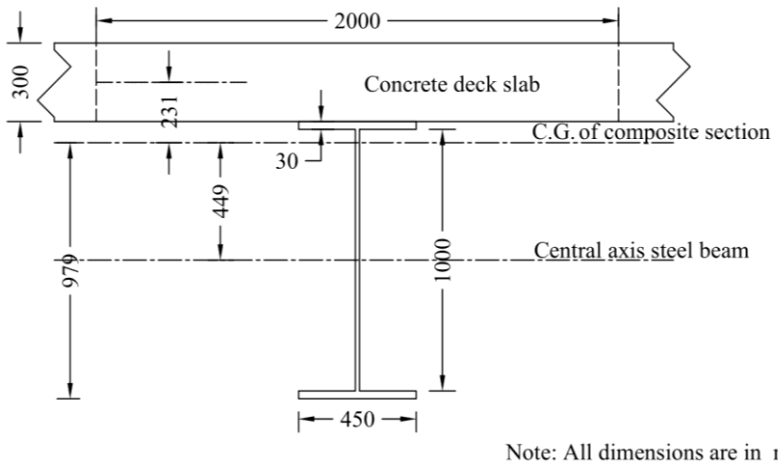

Fig. 2. Geometric and sectional properties of the steel-concrete composite I-girder section

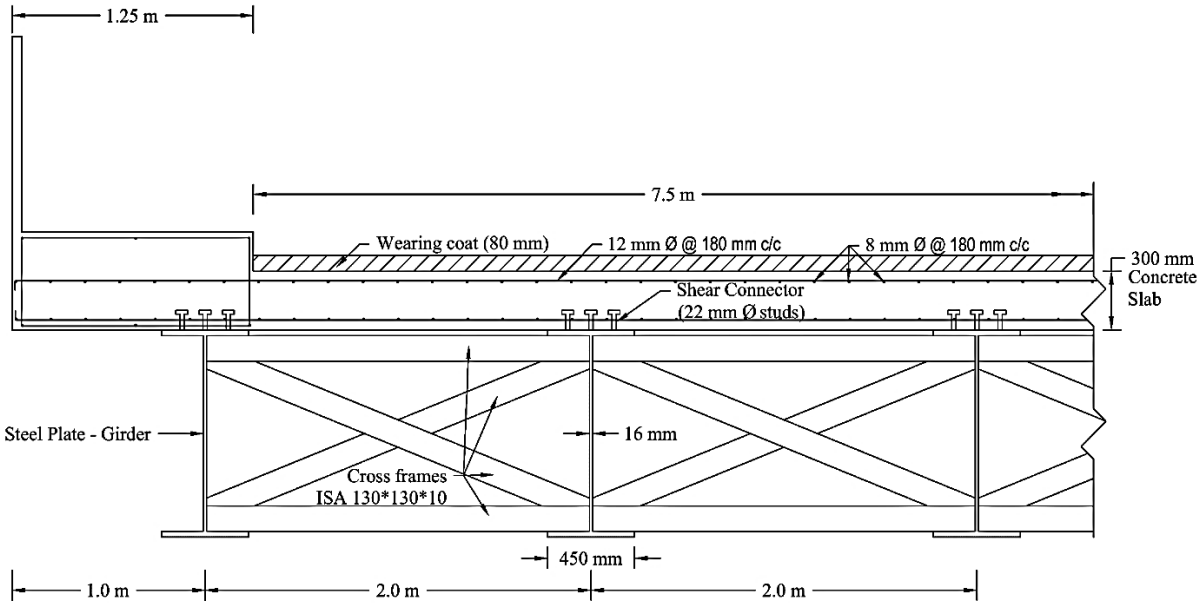

Fig.3 Cross section of the composite bridge superstructure

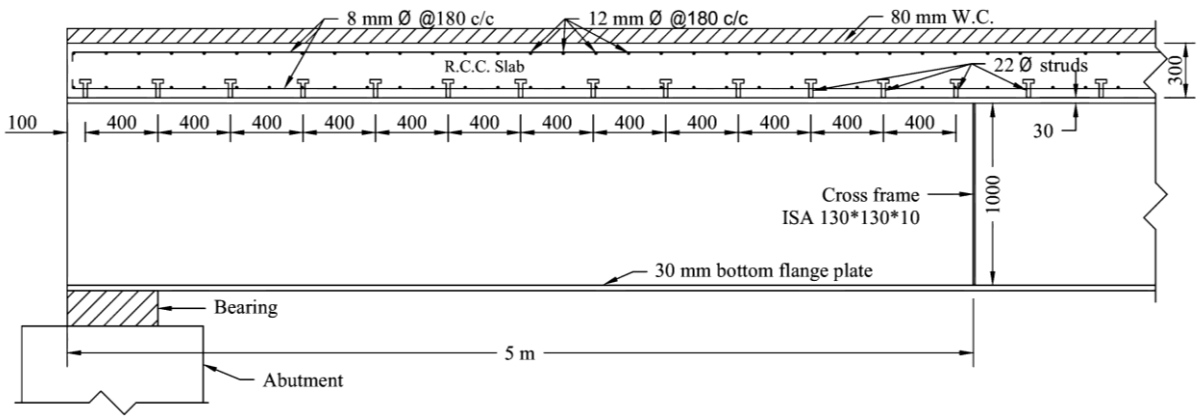

Fig. 4. Longitudinal section of the composite bridge superstructure

3.1.4 Finite Element Modeling

As per the material and section properties defined, the finite element model of the composite I-girder bridge is developed in MIDAS Civil using a three-dimensional grillage approach as portraited in Figure 5. Primary structural components, such as steel plate girders, cross bracings, and composite deck girder system, are modeled using frame (beam) elements as this modeling choice is well suited for capturing global flexure, shear, and torsion of girder bridges. The superstructure uses an average element length of about 1.0 m along the span. A mesh sensitivity study is conducted to refine the element size monitoring the key response quantities such as mid-span deflection, maximum bending moment, and shear force. The results showed negligible variation (less than 5%) between successive refinements and the final mesh balances numerical accuracy and computational efficiency for the analysis. The model is subjected to uniform 2% modal damping ratio enhanced by a multiplying factor of 1.6 in accordance with IRC:6-2017.

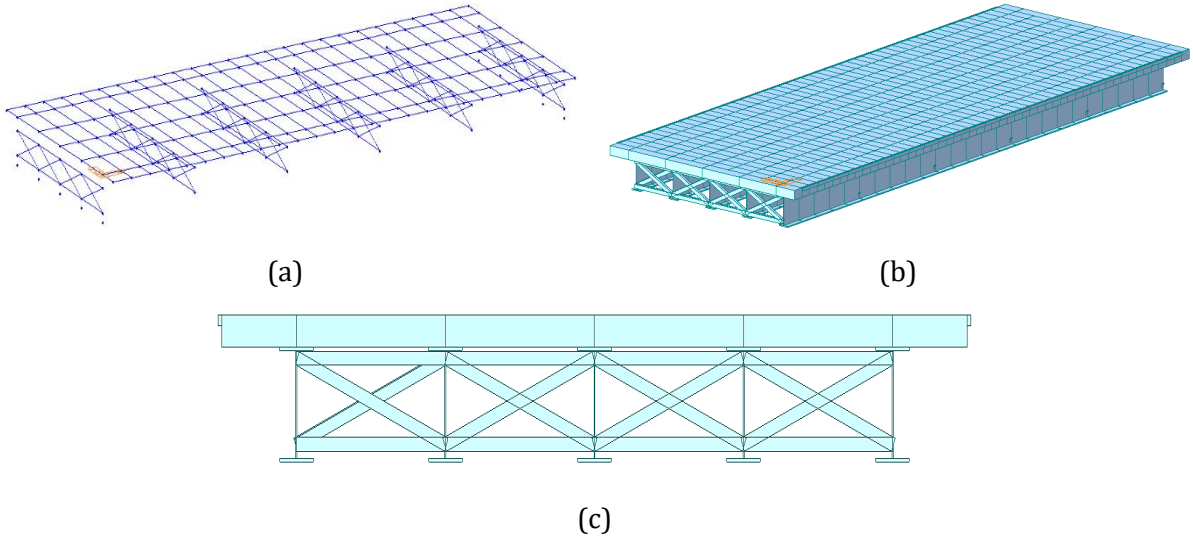

Fig. 5 Finite element model of the developed composite I-girder bridge superstructure (a) Grillage model, (b) 3D model and (c) Cross sectional view

3.1.5 Boundary Conditions

Firstly, to account for the rigid connection between the top slab and the girders, the nodes are connected using rigid links, which appropriately simulate relative deformation. Furthermore, the connection from the bottom of the girder to the bottom of the bearing (i.e., the top of the pier cap) is modeled using elastic links to represent the bearings themselves, with appropriate stiffness values assigned. Finally, since the substructure is not being modeled, the bottom of the bearings is assumed to be fixed. Therefore, fixed supports are assigned at these locations as shown in Figure 6, from which the reaction components can be extracted.

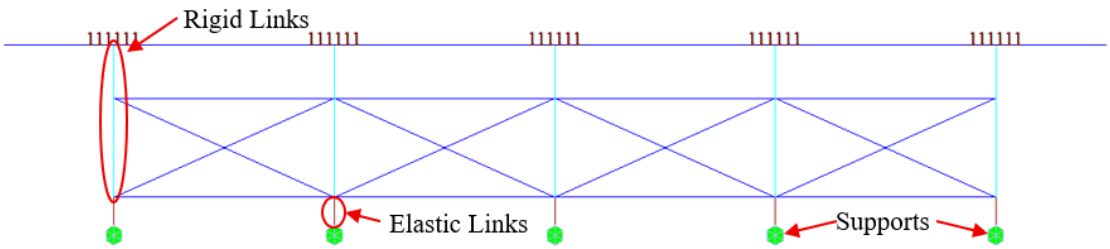

Fig. 6. Boundary condition idealization showing supports with rigid and elastic link

3.1.6 Dead loads

- Self-weight: Self-weight is applied to the analysis model using the self-weight command and with an option to adjust its intensity through a self-weight multiplier. The software calculates self-weight automatically from the defined section properties and material density in the model.

Self-weight factor = -1

- Super imposed dead load: In this model wearing course load and crash barrier loads are defined as the super imposed dead load. Wearing course load is computed as 3.52 kN/m/girder assuming the thickness of wearing course as 80 mm and unit weight of asphalt as 22 kN/m^3.

Crash Barrier load is assumed as 10 kN/m.

3.1.7 Formulation of Construction Stage

A series of staged analyses during finite element modeling captures the incremental changes in structural behavior during the construction stage of a steel-composite I-girder bridge. This process is divided into three distinct steps, each reflecting the activation or deactivation of structural elements, boundary conditions, and loads to closely simulate field operations.

- Stage 1: Activation of steel I-girders and bracings with permanent supports. Once these primary members and restraints are in place, the self-weight of the steel elements is applied as a dead load.
- Stage 2: Applying wet concrete load as a construction load for 14 days to simulate deck slab casting.
- Stage 3: The temporary green concrete load is deactivated and the deck slab elements are activated. Additionally, the final service stage loads such as, crash barrier load and wearing course load are then applied and the final stresses are checked for the long-term case.

3.1.8 Applied Loadings

The loads for the validation of the developed model are computed and applied as per the IRC 6, 2017, discussed as follows.

- Temperature Loads: As per clause 215 of IRC 6, 2017 temperature loads in the model are defined as the uniform temperature load and temperature gradient. The overall temperature change of the bridge over a specific period, will have a minimum and a maximum temperature range. Assuming the region of the bridge site as New Delhi the maximum and minimum temperature load is computed as 23.7°C ± 17.05°C as per clause 215.2 of IRC 6, 2017. And, the temperature gradient is the difference in temperature between the top surface of the bridge and the levels below it through the depth of the superstructure [12]. As per clause 215.3 the positive and reverse temperature gradient is computed as in Table 3 and 4.

Table 3. Calculation of positive temperature gradient

Segment	H1 (m)	H2 (m)	T1 (°C)	T2 (°C)
1	0	0.18	20.5	4
2	0.18	0.3	4	3.077
3	0.3	0.33	3.077	2.846
4	0.33	0.7	2.846	0.000

Note: Taking reference as top of the bridge.

Table 4. Calculation of reverse temperature gradient

Segment	H1 (m)	H2 (m)	T1 (°C)	T2 (°C)
1	0	0.18	-6.800	0.000
2	0.3	0.33	0.000	-0.600
3	0.33	0.7	-0.600	-8.000
4	0.7	1.36	-8.000	-8.000

Note: Taking reference as top of the bridge.

- Wind Load: Considering the terrain type as obstructive and assuming the height of pier including pier cap 7 m, the wind load for the developed model located at New-Delhi is computed and following results in Table 5 are obtained as per Section 209 IRC 6, 2017.

Table 5. Wind load on bridge structure

Wind Load Component	Intensity (kN/m)
Transverse force on SS (F_T)	4.204
Longitudinal force on SS (F_L)	1.051
Uplift force per girder (F_U)	1.159
Transverse force on Vehicle (F_{TL})	1.774
Longitudinal force on Vehicle (F_{LL})	0.443

- Static seismic Load: For Indian seismic zone IV (i.e. New Delhi) considering important seismic class and medium type of soil, static seismic load for the steel-composite bridge super-structure is analyzed as per section 218 IRC 6, 2017. The computed seismic demand due to live load and dead load are presented in Table 6 and 7 respectively.

Table 6. Seismic demand due to live load

Seismic Load Components	Intensity (kN/m/girder)
In longitudinal direction	0 (Cl. 218.5.2 IRC 6, 2017)
In transverse direction	0.893
In vertical direction	0.596

Table 7 Seismic demand due to dead loads

Seismic Load Components	Intensity (as factors of dead load)
In longitudinal direction	0.504
In transverse direction	0.504
In vertical direction	-0.336

- Vehicular Load: For a two-lane carriageway, two load cases must be evaluated: one scenario with a single lane loaded by a 70R vehicle, and another with both lanes subjected to Class A vehicle loading [12]. However, in this study class AA and special vehicle are also considered. Lanes are designated in the model for the live load cases, and the eccentricities for these lanes are calculated according to Table 6A of IRC 6, 2017, illustrated as follows in Table 8.

Table 8. Definition of lanes for moving loads

Vehicle Class	Lane	Wheel spacing (m)	Eccentricity from left edge of the bridge (m)
Class A	1	1.8	2.55
	2	1.8	6.05
Class 70R	1	2.06	3.9
Class AA	1	2.05	3.9
Special Vehicle	1	1.8	5.3

- Braking Load: The braking effect acting on a simply supported span is assumed as per the clause 211.2 IRC 6, 2017. The critical case in present scenario for braking load is the class 70R wheeled vehicle with vertical load 1000 kN among Class A, Class AA and Class 70R vehicles. Thus, braking load due to 70R vehicle is 20% of vertical load i.e. 20 kN (i.e. 1.6 kN/m/girder). And, the load has an eccentricity of 1.2 m acting along a line parallel to the roadway, as specified in clause 211.3 IRC 6, 2017.

3.1.9 Validation of the Bridge Model

To ensure the structure and its elements perform adequately throughout their service life, the serviceability limit states (i.e. stress level, deflection and crack width) shall have to be satisfied [17-19].

- Stress Limitation

a. In the concrete of the slab (Cl. 12.2.1, IRC 112, 2011)

The maximum stress (σ_c) = -7.72 MPa

$\leq 0.48 f_{ck}$. Hence, okay.

b. In the reinforcement steel (Cl. 12.2.2, IRC 112, 2011)

The maximum stress (σ_c) = -38.81 MPa

$\leq 0.8 f_y$. Hence, okay.

c. In the structural steel (C.4.3.1, IRC SP 120, 2018)

Nominal stress due to bending moment, (f_b) = 201.19 MPa

$\leq 0.87\ f_y / \gamma_{m,ser}$

Nominal stress due to shear, (τ_b) = 0.01 MPa

$\leq 0.87\ f_y / (\sqrt{3} \times \gamma_{m,ser})$

$\therefore$ Combined stress, $\sqrt{f_b^2 + 3\tau_b^2} = 201.19$ MPa

$\leq 0.87\ f_y / \gamma_{m,ser}$ Hence, okay.

- Deflection Control (Cl. 604.3.2 IRC 22, 2015)

a. Deflection of composite girder under dead, super-imposed & live load impact,

$d_{dl,ll} = -38.730\ mm \leq (L/600)$ Hence, okay.

where, L = Span of the girder

- Crack Width (Cl. 12.3.4, IRC 112, 2011)

a. Crack width at top

Stress at top surface, σ_{top} = -7.467 MPa. For compressive stresses, the crack check is skipped.

b. *Crack Width at bottom*

Stress at top surface, σ_{bottom} = -0.887 MPa. For compressive stresses, the crack check is skipped.

3.2 Dynamic Analysis

Dynamic analysis of the composite I-girder bridge superstructure focusing on its response under vehicular loading and earthquake-induced ground motions is performed. The analysis begins with the identification of the critical vehicle position, converted to equivalent static loads, and modeled as lumped masses. Further, Eigenvalue analysis is performed to find the natural frequencies and mode shapes of the structure. Finally, Response Spectrum Analysis is performed for Indian seismic zones IV and V, and Time History Analysis using three recorded ground motions to assess seismic response.

3.2.1 Identification of Critical Vehicle Position

In bridge design and analysis, the position of moving vehicular loads on the span governs the magnitude of bending moment and deflection at any section. To determine the critical vehicle position, moving load analysis is done that produces the absolute maximum bending moment and mid-span deflection. The critical vehicular position for all the vehicles used for the analysis are portrayed in Figure 7. Once the critical position is established, the full moving-load model is

replaced with an equivalent static load system that reproduces that worst-case effect. This equivalent static vehicular load typically consists of concentrated loads placed at the critical spacings.

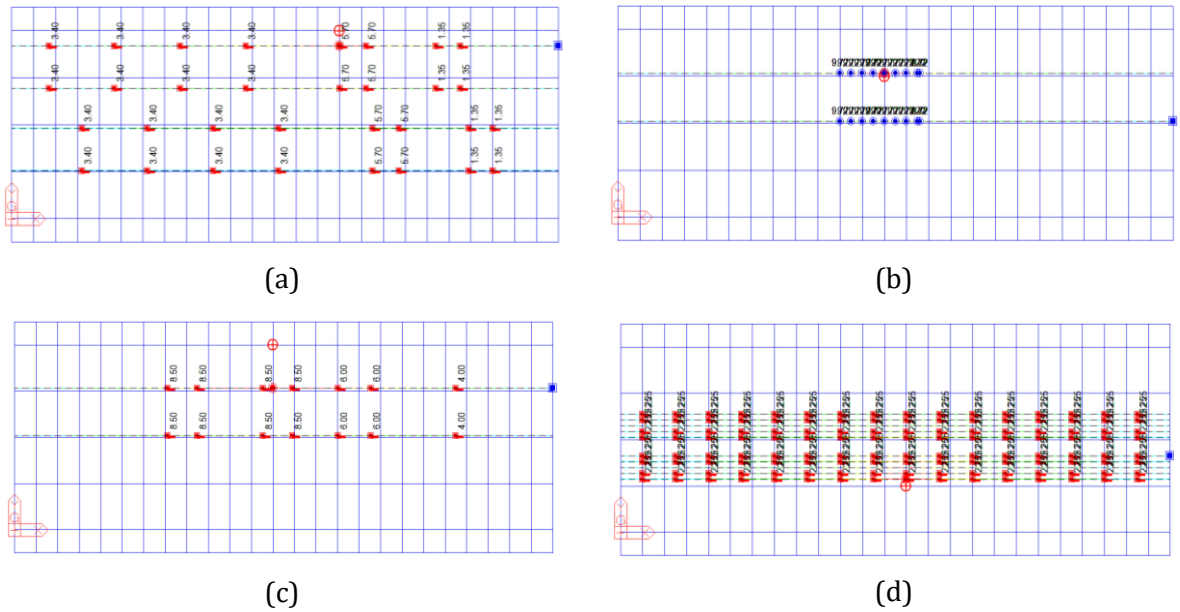

(a) (b)

(c) (d)

Fig. 7. Critical position of stationary IRC Vehicles on the bridge model(a) Dual class A, (b) Class AA (tracked), (c) Class 70R (wheeled) and (d) Special Vehicle

3.2.2 Application of Masses

Dynamic analysis is not performed using static loads directly, so each dead load and all other static load cases are firstly converted into equivalent nodal masses via the mass generation tool before carrying out any modal, response-spectrum, or time-history analysis. In this study, the "Load to Masses" function available in MIDAS Civil software is utilized to represent both the vehicular and structural masses.

3.2.3 Eigenvalue Analysis Control

Eigenvalue analysis determines a structure's dynamic properties by solving the characteristic equation composed of its mass and stiffness matrices. These properties include natural modes or mode shapes, natural periods or frequencies, and modal participation factors. The natural frequencies and corresponding periods are summarized in Table 9, while the modal participation masses of the developed bridge model are presented in Table 10.

Table 9. Natural frequency and period of the model

Mode No.	Natural Frequency (cycles / s)	Natural Period (s)	Mode No.	Natural Frequency (cycles / s)	Natural Period (s)
1.	3.493	0.286	11.	25.670	0.039
2.	4.379	0.228	12.	31.888	0.031
3.	10.743	0.093	13.	32.452	0.030
4.	12.297	0.081	14.	34.292	0.029
5.	12.486	0.080	15.	34.601	0.028
6.	14.953	0.066	16.	36.312	0.027
7.	19.629	0.050	17.	37.393	0.026
8.	20.944	0.047	18.	38.060	0.026
9.	22.329	0.044	19.	38.351	0.026
10.	23.026	0.043	20.	43.919	0.023

Table 10. Modal participation masses

Mode No.	Transverse-X		Transverse-Y		Transverse-Z		Rotation-X		Rotation-Y		Rotation-Z	
	Mass (%)	Sum (%)	Mass (%)	Sum (%)	Mass (%)	Sum (%)	Mass (%)	Sum (%)	Mass (%)	Sum (%)	Mass (%)	Sum (%)
1.	2.27	2.27	0.00	0.00	78.93	78.93	0.00	0.00	0.00	0.00	0.00	0.00
2.	0.00	2.27	0.11	0.11	0.00	78.93	78.63	78.63	0.00	0.00	0.11	0.11
3.	0.00	2.27	92.90	93.01	0.00	78.93	0.15	78.78	0.00	0.00	0.00	0.11
4.	9.64	11.91	0.00	93.01	0.12	79.05	0.00	78.78	51.97	51.97	0.00	0.11
5.	0.00	11.91	2.03	95.05	0.00	79.05	0.14	78.91	0.00	51.97	4.04	4.15
6.	0.12	12.03	0.00	95.05	0.03	79.08	0.00	78.91	0.51	52.48	0.00	4.15
7.	17.71	29.73	0.00	95.05	0.06	79.15	0.00	78.91	0.18	52.67	0.00	4.15
8.	0.00	29.73	0.06	95.11	0.00	79.15	0.93	79.84	0.00	52.67	78.26	82.41
9.	17.83	47.57	0.00	95.11	1.96	81.11	0.00	79.84	3.07	55.74	0.00	82.41
10.	0.00	47.57	0.32	95.43	0.00	81.11	8.39	88.24	0.00	55.74	12.72	95.13
11.	39.13	86.70	0.00	95.43	2.66	83.77	0.00	88.24	1.25	56.99	0.00	95.13
12.	0.00	86.70	0.06	95.49	0.00	83.77	0.01	88.25	0.00	56.99	0.16	95.29
13.	0.73	87.42	0.00	95.49	0.03	83.80	0.00	88.25	7.22	64.21	0.00	95.29
14.	7.78	95.20	0.00	95.49	4.32	88.12	0.00	88.25	0.52	64.73	0.00	95.29
15.	0.00	95.20	0.38	95.87	0.00	88.12	0.00	88.25	0.00	64.73	0.00	95.29
16.	0.00	95.20	2.41	98.28	0.00	88.12	0.39	88.64	0.00	64.73	0.01	95.30
17.	0.00	95.20	0.13	98.41	0.00	88.12	0.11	88.75	0.00	64.73	0.25	95.55
18.	0.37	95.58	0.00	98.41	1.46	89.58	0.00	88.75	0.04	64.78	0.00	95.55
19.	0.00	95.58	1.25	99.65	0.00	89.58	1.91	90.66	0.00	64.78	0.02	95.57
20.	0.00	95.58	0.03	99.68	0.00	89.58	0.02	90.68	0.00	64.78	0.33	95.90

3.2.4 Response Spectrum Cases

This study performs response spectrum analysis for the seismic zones IV and V with zone factors 0.24 and 0.36 (Table 16, IRC 6, 2017) respectively considering the medium type of soil, importance factor 1.2 (Table 19, IRC 6, 2017) and response reduction factor as 1 (Table 20, IRC 6, 2017). Damping factor is taken as 2% for composite structure with a multiplying factor of 1.4 (Table 18-IRC 6, 2017). Both the cases are analyzed considering all the vehicular loads as per IRC 6, 2017. The response spectra used for seismic analysis in Zones IV and V are shown in Figure 8.

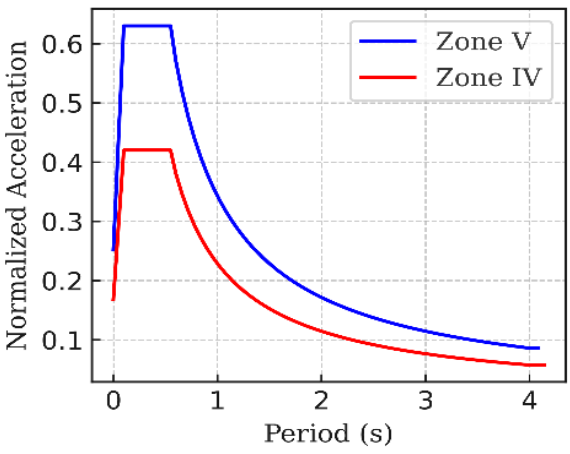

Fig. 8. Design response spectra for Indian seismic Zones IV and V

3.2.5 Time History Cases

Time History Analysis (THA) was performed for three cases corresponding to the Indian seismic Zone V, as summarized in Table 11. The earthquake acceleration records were obtained from the Strong Motion Virtual Data Center [20], and the corresponding accelerograms for each case are presented in Figures 9–11. This study excludes the vertical component of seismic motion as vertical peak ground acceleration is usually lower than the horizontal components and shows limited spectral amplification. Structural systems also have high vertical stiffness from gravity loads, which restricts vertical displacements and limits their impact on seismic response. And hence, only horizontal components are considered additionally improving computational efficiency.

Table 11. Time history cases

Earthquake	Station	Magnitude	Hypocentral distance (km)	Component	Peak ground acceleration (m/s²)
Bhuj/Kachchh 2001-01-26 03:16:40	Ahmedabad, Gujarat	7.0	239.0	Longitudinal (78)	-1.0382
				Transverse (348)	-0.78236
Chamoli 1999-03-28 19:05:11	Gopeshwar, Uttarakhand	6.6	17.3	Longitudinal (20)	-3.5283
				Transverse (290)	1.9507
India – Burma Border 1995-05-06 01:59:07	Diphu, Assam	6.4	245.6	Longitudinal (180)	1.0030
				Transverse (90)	0.78988

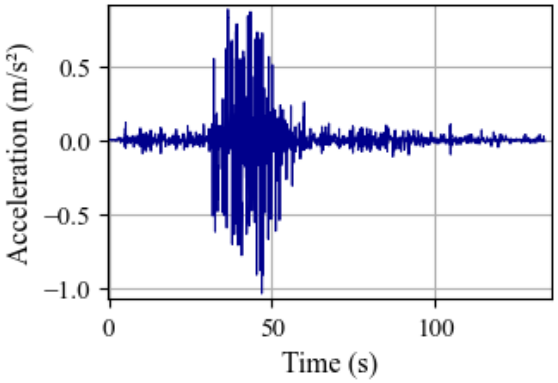

(a) Longitudinal

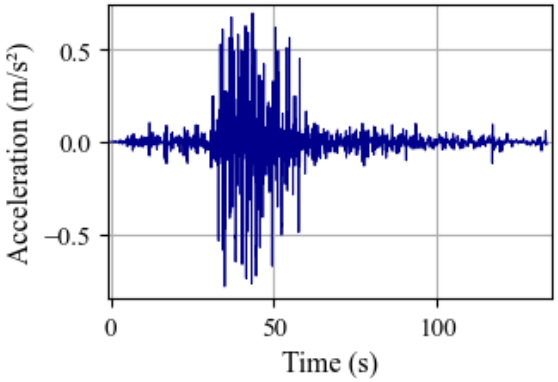

(b) Transverse

Fig. 9. Accelerogram of Bhuj/Kachchh earthquake

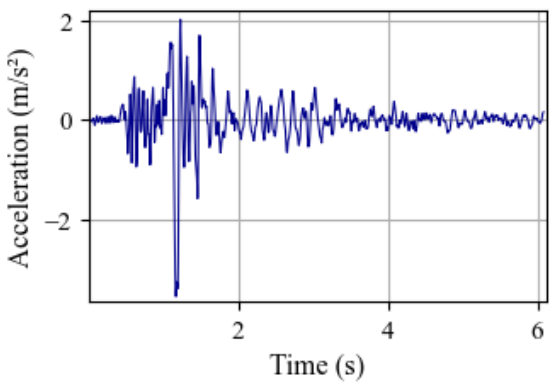

(a) Longitudinal

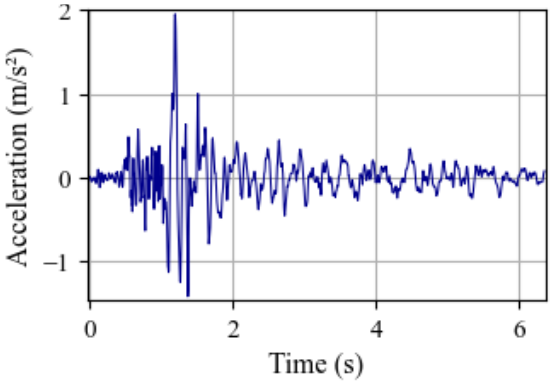

(b) Transverse

Fig. 10. Accelerogram of Chamoli earthquake

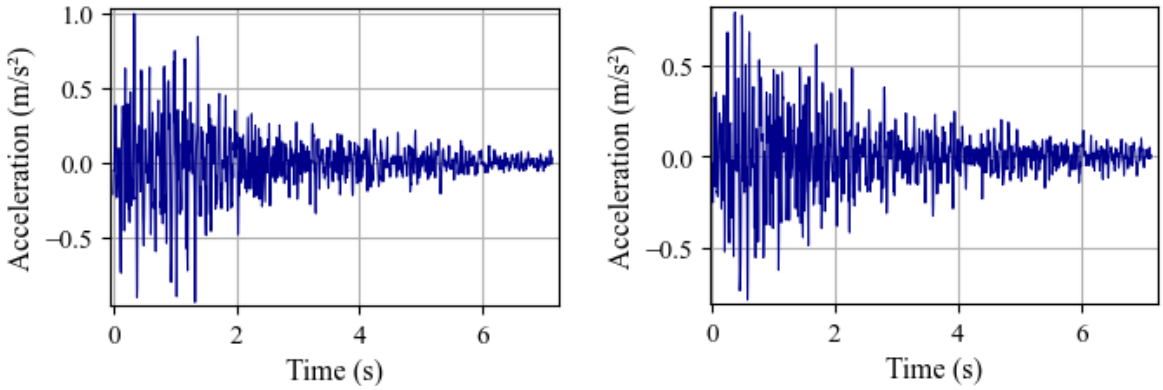

(a) Longitudinal (b) Transverse

Fig. 11. Accelerogram of India - Burma Border earthquake

4. Results and Discussions

The comparative assessment of the bridge's seismic response under different vehicular load scenarios, employing both Response Spectrum Analysis (RSA) and Linear Time History Analysis (THA), reveals consistent patterns in the increase of structural demand caused by the presence of heavy vehicles at mid-span. In all seismic scenarios, findings indicate that vehicular loading enhances deflection, shear force, and the bending moment, with the degree of increase proportional to the vehicle's total axle load. This supports earlier studies on vehicle-bridge interaction Ghosh et al. [1], Kameshwar & Padgett [4], Liu et al. [5], and additionally measures the impact in relation to IRC-specified loads and Indian seismic conditions.

4.1 Response Spectrum Analysis Results

In both Seismic Zones IV and V, RSA outcomes (Figures 12-14) show a clear monotonic relationship between axle load and structural response. The special vehicle with an effective axle load of 288 tons consistently caused the largest increases across all three response parameters. With special vehicle, in Zone IV, shear force increased by 115%, bending moment increased by 112%, and the deflection increased by 106% compared to the case without any vehicle. The amplification is stronger in Zone V, with responses about 50% higher than those in Zone IV. However, the percentage increases caused by the presence of vehicles compared to the unloaded case were similar in both zones. The increase in axle load shows increment in structural response however the relation is not linear as the rate of increase reduces in the case of IRC special vehicle.

Table 12. Summary of response spectrum analysis

Vehicle	Total axle load on bridge (tons)	Zone IV			Zone V		
		Max. shear force (kN)	Max. bending moment (kN-m)	Max. deflection (mm)	Max. shear force (kN)	Max. bending moment (kN-m)	Max. deflection (mm)
Without Vehicle	-	38.4	137.5	1.869	57.6	206.3	2.804
Class AA (Tracked)	70	44.1	191.8	2.632	66.1	287.7	3.948
Class 70R (Wheeled)	100	50.7	222.1	3.008	76.1	333.2	4.511
Dual Class A	2 * 55.4 = 110.8	57.1	233.6	3.156	85.7	350.5	4.734
Special Vehicle	288	82.4	290.8	3.855	123.6	436.2	5.828

Note: Although the total axle load of the special vehicle is 385 tons, only 288 tons is considered in analysis since its length (38.459 m) exceeds the bridge length (25 m).

This is probably due to differences in how the load is distributed. These results show that axle configuration and spacing matter as much as the total load in affecting dynamic demand. This acknowledges with Liu et al. [5], who highlighted how load distribution impacts structural response.

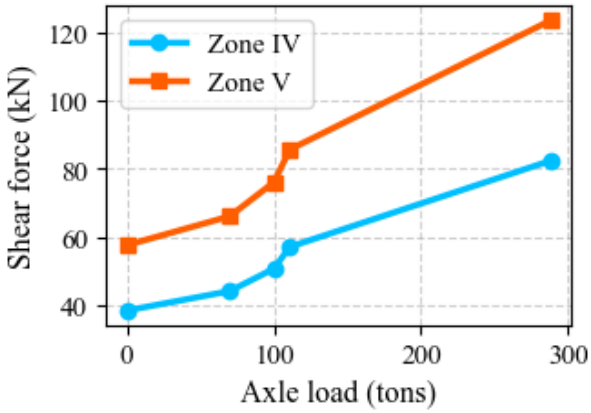

Fig. 12. Variation of shear force with axle load in seismic zones IV and V

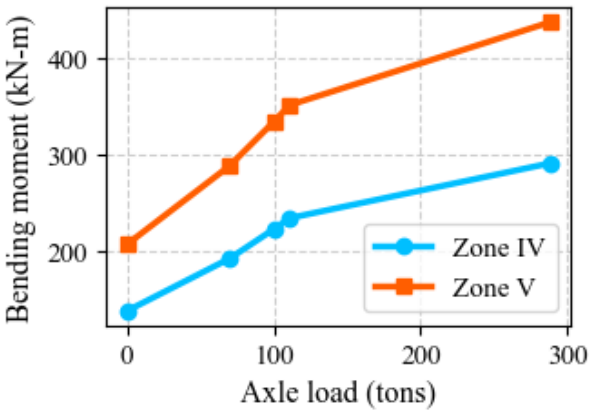

Fig. 13. Variation of bending moment with axle Load in seismic zones IV and V

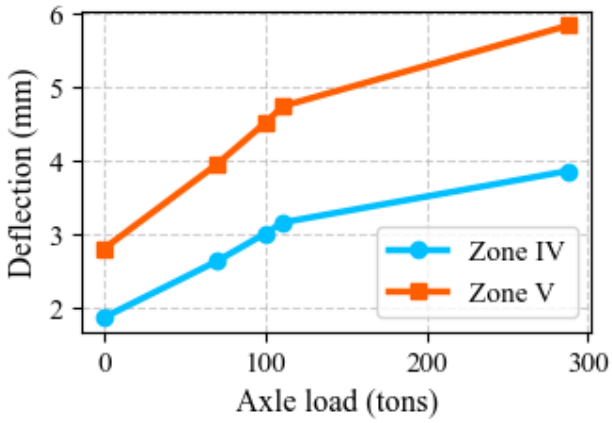

Fig.14. Variation of deflection with axle load in seismic zones IV and V

4.2 Time History Analysis Results

THA results (Figure 15-17) confirm the load-response relationship and also highlight how strongly earthquake record characteristics affect absolute demand values. The Chamoli earthquake, with its high PGA and close proximity, produced the highest responses across all load cases, which is 2 to 3 times higher than in the Bhuj or India-Burma border cases. This shows that short duration ground motions with high intensity can increase the negative impact of live loads. The results are in good agreement with the findings of Lin et al. [8] and Liu et al. [10] that near-fault motions with strong velocity pulses amplify structural responses more than far-field motions.

In the Bhuj earthquake case, the overall values were lower however the percentage increase caused by vehicles was still significant. For instance, the Special Vehicle increased bending moment from 119.9 kN-m (unloaded) to 216.5 kN-m which is about an 80% rise. In the India-Burma border case, some unexpected patterns appeared, such as the Special Vehicle producing lower deflection than lighter loads in certain situations. This likely happened because of complex interactions between vibration modes and timing differences between inertial forces and ground motion.

Figures 18-20 shows the displacement-time history plot of the different earthquakes and its variation in presence of loading conditions. The displacement-time history response for all loading conditions exhibits a fundamentally similar oscillatory behavior, characterized by a consistent harmonic motion around the neutral axis. However, the displacement amplitude varies significantly as per the loading conditions. This indicates that the natural frequency and damping

properties of the structure itself control the dynamic response. While the presence of varying vehicular loads alters the intensity of the oscillations, it does not significantly modify the fundamental pattern of structural vibration.

Table 13. Summary of time history analysis

Vehicle	Bhuj/Kachchh Earthquake			Chamoli Earthquake			India-Burma Border Earthquake		
	Max. SF (kN)	Max. BM (kN-m)	Max. Def. (mm)	Max. SF (kN)	Max. BM (kN-m)	Max. Def. (mm)	Max. SF (kN)	Max. BM (kN-m)	Max. Def. (mm)
No Vehicle	26.0	119.9	1.745	29.3	216.0	2.710	32.1	118.8	1.516
Class AA (Tracked)	33.7	144.0	2.273	74.3	533.8	8.189	75.9	229.3	3.680
Class 70R (Wheeled)	42.8	182.8	2.800	88.4	528.6	8.281	59.3	221.0	3.730
Dual Class A	44.3	176.4	2.793	92.0	623.4	8.932	59.1	288.9	4.049
Special Vehicle	55.9	216.5	2.836	96.1	592.9	9.016	80.6	199.5	2.777

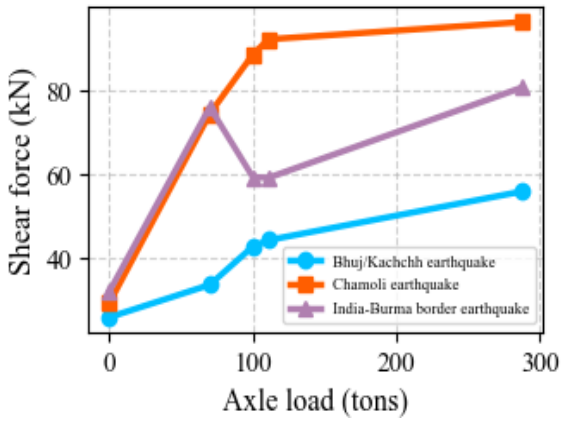

Fig. 15. Variation of shear force with axle load in different seismic events

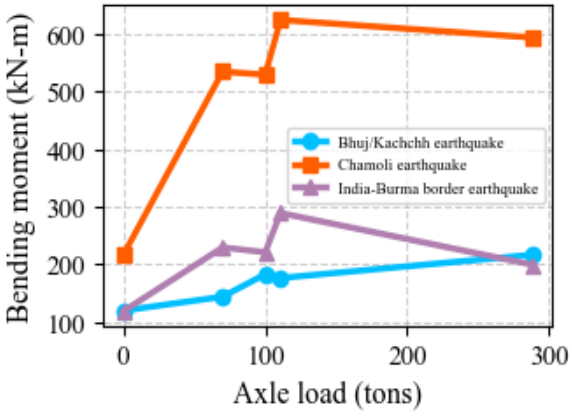

Fig. 16. Variation of bending moment with axle load in different seismic events

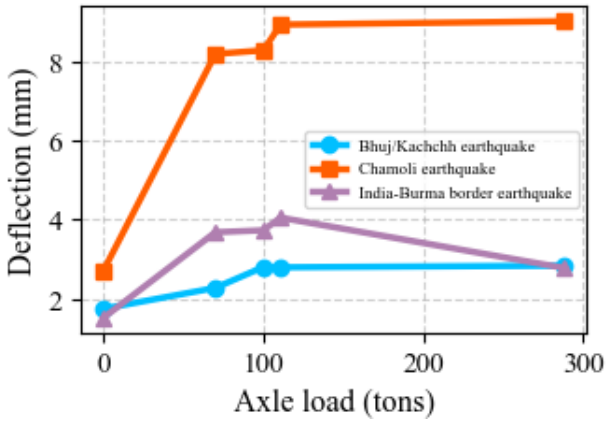

Fig. 17. Variation of deflection with axle load in different seismic events

In addition, the seismic performance of bridge structures is governed not only by the intensity of ground motion but also by inherent structural characteristics such as lateral strength, stiffness

distribution, and energy dissipation capacity. Implementing seismic isolation systems can significantly reduce seismic demands by increasing the fundamental period and providing additional damping, which in turn limits the forces transmitted to the superstructure [21–23]. At the same time, the seismic response is highly sensitive to material properties, reinforcement detailing as these factors influence stiffness degradation, ductility, and the progression of damage under cyclic loading [24]. Therefore, with a balanced combination of global response-control strategies and careful local detailing adequate seismic resilience can be achieved.

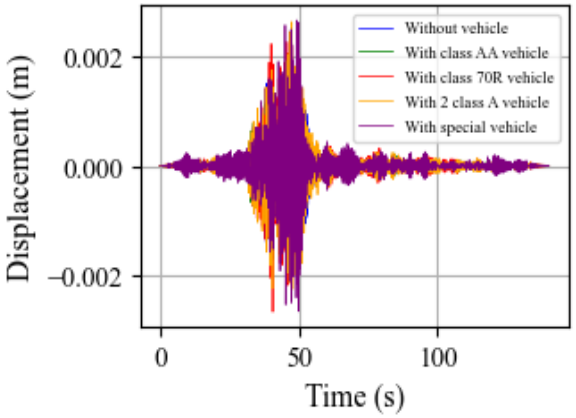

Fig. 18. Displacement time history of Bhuj/Kachchh earthquake

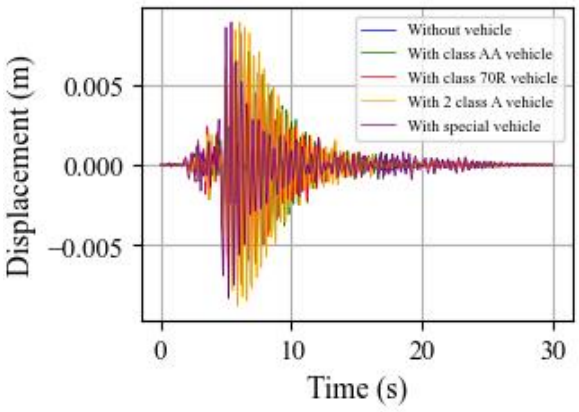

Fig. 19. Displacement time history of Chamoli earthquake

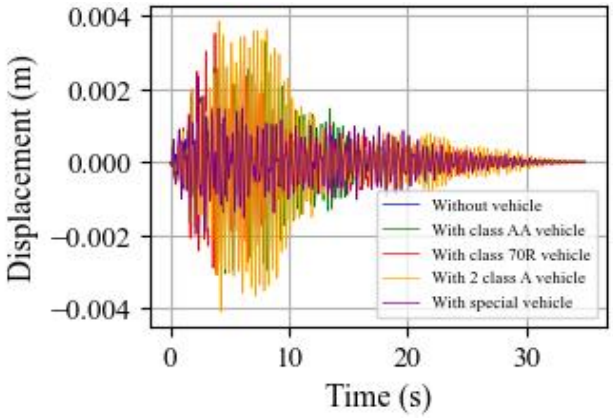

Fig.20. Displacement time history of India-Burma Border earthquake

5. Conclusions

This study analyzed the seismic response of a steel-concrete composite I-girder bridge in the presence of heavy vehicle utilizing both Response Spectrum Analysis (RSA) and Linear Time History Analysis (THA). RSA covers Indian seismic Zones IV and V. THA uses recorded ground motions from Bhuj Kachchh 2001, Chamoli 1999, and the India Burma Border 1995. The study evaluates several vehicular loading cases defined by the Indian Roads Congress. These include an unloaded bridge, Class AA Tracked, Class 70R Wheeled, dual Class A, and Special Vehicle configurations.

The results show that the presence of stationary vehicles during seismic events increase shear force, bending moment, and deflection compared to an unloaded bridge condition. Heavier axle loads and closer axle spacing generally lead to greater amplification, underscoring the importance of accounting for traffic conditions in seismic bridge analysis. In RSA, Zone V responses were about 50% higher than Zone IV for both loaded and unloaded conditions, showing the importance of region-specific seismic provisions.

THA results showed that the response depends strongly on the ground motion characteristics. The Chamoli earthquake, with its near-field effects, produced peak responses up to three times higher than the Bhuj/Kachchh and India-Burma border events, especially with heavy vehicles. This behavior emphasizes the critical role of near-field effects and frequency content in governing seismic demand. The Special Vehicle often produced the highest shear forces, yet depending on ground acceleration, dual Class A or Class 70R loads sometimes caused larger deflections or bending moments. This highlights the complex interaction between vehicle configuration, bridge dynamics, and seismic input.

Both RSA and THA showed that vehicles increase seismic demands, but THA usually gave higher peaks and captured interaction effects missed by RSA, making it more useful for assessing performance for near field earthquakes. The correlation between axle load and seismic response was strong but non-linear, affected by axle spacing and load distribution.

Overall, the results show that ignoring the combined effects of traffic loads and earthquakes leads to unconservative bridge designs. In moderate to high seismic regions, design practice should include the simultaneous action of vehicles and seismic excitation. This approach improves structural safety, serviceability, and resilience of critical transportation infrastructure.

6. Limitations

This study considered only single-span composite I-girder bridge with stationary mid-span vehicles under three Indian ground motions and two seismic zones. Traffic movement, wider seismic datasets, nonlinear effects, soil-structure interaction, and bearing damage were not modeled.

Acknowledgement

We are grateful to Andhra University College of Engineering (A), Visakhapatnam, for their guidance and support. We also express our deep appreciation to the Republic of India and Federal Democratic Republic of Nepal for enabling this journey through the Dr. Homi Jahangir Bhabha Scholarship Scheme (HJBSS). We sincerely thank Mr. Shishir Poudel and Mr. Anish Khanal for their technical guidance.

References

[1] Ghosh J, Caprani CC, Padgett JE. Influence of traffic loading on the seismic reliability assessment of highway bridge structures. Journal of Bridge Eng. 2013;19(3):04013003. https://doi.org/10.1061/(ASCE)BE.1943-5592.0000535

[2] Borjigin S, Kim CW, Chang KC, Sugiura K. Non-linear seismic response analysis of vehicle-bridge interactive systems. Struct Control Health Monit. 2015;22(9):1110–25. https://doi.org/10.1002/stco.201510006

[3] Shaban N, Caner A, Yakut A, Askan A, Karimzadeh Naghshineh A, Domanic A, Can G. Vehicle effects on seismic response of a simple-span bridge during shake tests. Earthquake Eng Struct Dyn. 2015;44(5):889–905. https://doi.org/10.1002/eqe.2491

[4] Kameshwar S, Padgett JE. Effect of vehicle bridge interaction on seismic response and fragility of bridges. Earthquake Eng Struct Dyn. 2017;47(3):713–35. https://doi.org/10.1002/eqe.2986

[5] Liu L, Yang X, Yan B, Miao S. Dynamic responses of RC girder bridge under heavy truck and seismic loads combined. Sustainability. 2022;14(15):9263. https://doi.org/10.3390/su14159263

[6] Fu G, Feng J, Dekelbab W, Moses F, Cohen H, Mertz D. Impact of commercial vehicle weight change on highway bridge infrastructure. J Bridge Eng. 2008;13(6):556–64. https://doi.org/10.1061/(ASCE)1084-0702(2008)13:6(556)

[7] Itani AM, Bruneau M, Carden L, Buckle IG. Seismic behavior of steel girder bridge superstructures. J Bridge Eng. 2004;9(3):243–9. https://doi.org/10.1061/(ASCE)1084-0702(2004)9:3(243)

[8] Lin Y, Bi K, Zong Z, Hao H, Lin J, Chen Y. Seismic performance of steel–concrete composite rigid-frame bridge: Shake table test and numerical simulation. J Bridge Eng. 2020;25(7):04020043. https://doi.org/10.1061/(ASCE)BE.1943-5592.0001558

[9] Wang T, Xie X, Cheng C. Probabilistic seismic demand analysis for bridges based on earthquake scenarios. Eng Struct. 2025;323:119128. https://doi.org/10.1016/j.engstruct.2024.119128

[10] Liu X, Li L, Liu Y, Chen S, An W. Study on the influence of near-fault vertical ground motion on the dynamic response of separation and collision of bridge. Sci Rep. 2025;15:36372. https://doi.org/10.1038/s41598-025-20347-5

[11] Ramadan OMO, Mehanny SSF, Kotb AAM. Assessment of seismic vulnerability of continuous bridges considering soil–structure interaction and wave passage effects. Eng Struct. 2020;206:110161. https://doi.org/10.1016/j.engstruct.2019.110161
[12] Indian Roads Congress. IRC 6-2017: Standard specifications and code of practice for road bridges—Section II: Loads and load combinations. 7th rev. New Delhi: Indian Roads Congress; 2017.
[13] American Association of State Highway and Transportation Officials. AASHTO LRFD bridge design specifications. 8th ed. Washington, DC: AASHTO; 2017.
[14] European Committee for Standardization. EN 1991-2: Eurocode 1: Actions on structures—Part 2: Traffic loads on bridges. Brussels: CEN; 2003.
[15] American Association of State Highway and Transportation Officials. AASHTO guide specifications for LRFD seismic bridge design. 2nd ed. Washington, DC: AASHTO; 2011.
[16] European Committee for Standardization. EN 1998-2: Eurocode 8: Design of structures for earthquake resistance—Part 2: Bridges. Brussels: CEN; 2005.
[17] Indian Roads Congress. IRC 112-2011: Code of practice for concrete road bridges. New Delhi: Indian Roads Congress; 2011.
[18] Indian Roads Congress. IRC 22-2015: Standard specifications and code of practice for concrete road bridges—Section VI: Composite construction (limit state design). New Delhi: Indian Roads Congress; 2015.
[19] Indian Roads Congress. IRC SP:120-2018: Explanatory handbook to IRC:22-2015. New Delhi: Indian Roads Congress; 2018.
[20] Center for Engineering Strong Motion Data (CESMD). Strong Motion Virtual Data Center. Available from: http://www.strongmotioncenter.org [Accessed 19 Jun 2025].
[21] Soneji B B, Jangid R S. Effectiveness of seismic isolation for cable-stayed bridges. Int. J. Struct. Stab. Dyn. 2006;6(1):77–96. https://doi.org/10.1142/S0219455406001836
[22] Patel D, Mourya VK, Pandey G, Kumar P. Advancements in base isolation for seismic mitigation: Perspectives on elastomeric and lead rubber bearings. Res. Eng. Struct. Mater., 2024; 10(3): 1017-1049. https://doi.org/10.17515/resm2024.15ma0927rv
[23] Jangid R S. Seismic performance assessment of clutching inerter damper for isolated bridges. Pract. Period. Struct. Des. Constr., 2022;27(2):04021078. https://doi.org/10.1061/(ASCE)SC.1943-5576.0000661
[24] Ozmen H B, Inel M. Effect of concrete strength and detailing properties on seismic damage for RC structures. Research and Design. 2024;1(1):1–11. https://doi.org/10.17515/rede2024-005en1124rs